A theoretical study of CH4 dissociation on pure and gold-alloyed Ni(111) surfaces

Kratzer, P.; Hammer, Bjørk; Nørskov, Jens Kehlet

Published in:
Journal of Chemical Physics

Link to article, DOI:
10.1063/1.472399

Publication date:
1996

Document Version
Publisher's PDF, also known as Version of record

A theoretical study of CH_4 dissociation on pure and gold-alloyed Ni(111) surfaces

P. Kratzer
Center for Atomic-scale Materials Physics and Physics Department, Technical University of Denmark, DK-2800 Lyngby, Denmark and Physik-Department, Technische Universität München, D-85747 Garching, Germany

B. Hammer
National Center for Supercomputing Applications, University of Illinois at Urbana-Champaign, Urbana, Illinois 61801 and Joint Research Center for Atom Technology (JRCAT), 1-1-4 Higashi, Tsukuba, Ibaraki 305, Japan

J. K. Nørskov
Center for Atomic-scale Materials Physics and Physics Department, Technical University of Denmark, DK-2800 Lyngby, Denmark

(Received 25 April 1996; accepted 21 June 1996)

We present a density functional theory study of the first step of CH_4 adsorption on the Ni(111) surface, dissociation into adsorbed CH_3 and H. The rupture of the C–H bond occurs preferentially on top of a Ni atom, with a dissociation barrier of about 100 kJ/mol (including zero point corrections). The transition state involves considerable internal excitation of the molecule. The active C–H bond is both stretched to 1.6 Å and tilted relative to the methyl group. A normal mode analysis shows that the reaction coordinate is mainly a C–H stretch, while the orientation of the C–H bond relative to the surface is responsible for the highest real mode. Alloying the surface with gold also affects the reactivity of the Ni atoms on adjacent surface sites. The dissociation barrier is increased by 16 and 38 kJ/mol for a Ni atom with one or two gold neighbors, respectively. We attribute these changes to a shift in the local density of d states at the nickel atoms in the neighborhood of gold. © *1996 American Institute of Physics.* [S0021-9606(96)02136-8]

I. INTRODUCTION

The breaking of a C–H bond in methane is the key to transform the resources of natural gas into useful products like hydrogen and petrochemicals. However, the high stability of methane makes the C–H bond activation a challenging technological problem. Industrially a nickel catalyst is used to transform methane into hydrogen and carbon monoxide in the catalytic steam reforming process.[1] The dissociative adsorption of CH_4 is thought to be the rate limiting step in this reaction. Due to its industrial importance, much experimental as well as theoretical work has been devoted to an understanding of the dissociation and chemisorption of methane on nickel surfaces.

Experimentally, seeded molecular beam experiments offer the possibility to gain insight into the details of dissociative adsorption of CH_4. Such experiments were performed for the Ni(111)[2,3] and also for the Ni(100)[4,5] surface. Ceyer and co-workers[2,6] used electron energy loss spectroscopy to probe the adsorbed fragments, and attributed the features in the loss spectra to adsorbed CH_3 as the primary product of the reaction. In the regime of low sticking factors ($s<10^{-3}$), an exponential increase of the sticking with the translational energy of the molecules normal to the surface is observed for both Ni(111) and Ni(100). This suggests that the dissociation of CH_4 on these surfaces is a direct, highly activated process. However, the sticking coefficient on Ni(100) is found to be an order of magnitude higher than on Ni(111).[3] Besides the translational energy in the beam, internal excitation of the CH_4 molecule is apparently a key factor determining the sticking coefficient. The importance of internal excitations was attributed to a sizable stretch of the C-H bond at the transition state. Such an interpretation was corroborated by calculations of the dynamics of CH_4 dissociation on model potential energy surfaces.[7,8] Additional information about the activated adsorption of CH_4 can be obtained from high pressure experiments. Here a gas containing CH_4 is in equilibrium with the adsorbate on a nickel surface. The temperature dependence of adsorption is often expressed as an apparent activation energy. Beebe *et al.* studied the Ni(100), Ni(110), and Ni(111) surfaces in this way and obtained activation energies of 27, 58, and 53 kJ/mol, respectively.[9] In a later experiment, however, Chorkendorff *et al.*[10] reported an activation energy of 52 kJ/mol for the Ni(100) surface. In view of this experimental result, it appears plausible that the physics of CH_4 dissociation is similar on all low-index nickel surfaces. By using mixtures of CH_4 with different buffer gases, Hanley, Xu, and Yates[11] showed that CH_4 adsorption on the Ni(111) surface is a direct process also at high pressures, and that translational and vibrational excitations of the molecule are both kinetically important.

Due to its importance for catalysis, there is a rich literature of theoretical studies related to CH_4 dissociation. Early work concentrated on the insertion of a single Ni atom into a C–H bond in methane[12] or followed a semiempirical approach to cluster models of adsorption.[13] Several *ab initio*

studies addressed the chemisorption of CH_3 on the Ni(111) surface modeled by medium-sized clusters.[14,15] In recent years, Yang and Whitten treated the dissociative chemisorption of CH_4 on Ni(111) in a large cluster model at the CI (configuration interaction) level.[16] They report a barrier of 71 kJ/mol for adsorption of CH_3 and H into separated threefold hollow sites. Burghgraef, Jansen, and van Santen studied both the insertion of a Ni atom[17] and the dissociation of CH_4 on various clusters[18,19] within the framework of density functional theory. They observe that calculated barrier heights in their cluster models are very sensitive to the cluster size, ranging from 214 kJ/mol for a Ni_7 cluster to 121 kJ/mol for a Ni_{13} cluster, but generally higher than the barrier for Ni atom insertion, which they determined to be 41 kJ/mol. In a recent study of the dynamics of CH_4 dissociation on Ni(111),[20] Jansen and Burghgraef argue that the Ni_{13} cluster is probably closer to the physical properties of a real surface than the Ni_7 cluster. For the dynamics they assumed a barrier of 93.2 kJ/mol in order to obtain quantitative agreement with experimental sticking data. For comparison it should also be noted that Swang and co-workers[21] found a barrier in the range of 63–71 kJ/mol for the Ni(100) surface treated as a Ni_{13} cluster on the *ab initio* CI level.

In this paper, we report density functional calculations of CH_4 dissociation for a slab model of the Ni(111) surface. We discuss the reaction pathway and determine the normal modes at the transition state. The consequences of the calculated potential and its relation to the experimental data is also briefly discussed. Finally, we calculate the adsorption barrier for different atomic sites in a disordered surface alloy of nickel with gold. We demonstrate that the barrier height is sensitive to the local environment of the active nickel atom.

II. CALCULATIONS

Potential energies for a CH_4 molecule dissociating over Ni(111) are obtained by means of total energy calculations using pseudopotentials in connection with a plane wave basis set. The substrate is represented by a rigid Ni slab of the truncated bulk geometry at the calculated equilibrium lattice constant $a_0 = 3.47$ Å. Unless otherwise stated, the results refer to a four layer slab with a lateral unit cell consisting of four Ni atoms. This corresponds to a distance between CH_4 molecules in neighboring unit cells of 4.9 Å . 18 k points are used to sample the whole Brillouin zone [3 (6) **k** points in the C_{3v} (C_{2v}) irreducible part of the Brillouin zone]. Several test calculations for selected configurations are performed for a slab with six Ni layers. For improved convergence a Brillouin zone sampling with 54 points in total is used [6 (15) **k** points in the C_{3v} (C_{2v}) irreducible part of the Brillouin zone].

The exchange and correlation effects within the electron system are described in the density functional theory approach. In particular, we use the gradient corrected functional of Perdew and co-workers (GGA-II),[22] applied to an electronic density which has been calculated self-consistently using the local-density approximation[23,24] for exchange and correlation. The Kohn–Sham equations are solved by alternating conjugate gradient minimizations of the total energy[25] and subspace rotations.[26] Occupation numbers are found according to a Fermi-function distribution. In order to stabilize the numerical procedures, a fictive electronic temperature is introduced. A value of $k_BT = 0.3$ eV and $k_BT = 0.1$ eV is used for the 4-layer slabs and the 6-layer slabs, respectively. All total energies are extrapolated to zero electronic temperature.[26]

To describe the Ni and C atoms we use pseudopotentials constructed in the way suggested by Troullier and Martins.[27] For Ni, the $3d$, $4s$, and $4p$ states are included, with $r_c = 2.08$, 2.30, and 2.08 bohr for s,p and d, respectively. The $4p$ potential is constructed from the excited ionic configuration $Ni^+(4s^{0.75}3d^84p^{0.25})$. The pseudopotential for carbon includes the $2s$ and $2p$ valence states, with $r_c = 1.50$ and 1.54 bohr, respectively. The pseudopotentials are brought to the fully separable Kleinman–Bylander form.[28] As the local part of the potential we use the potential in the $4s$ channel for Ni, and the $2p$ channel for C. Hydrogen is described by its full Coulombic potential. Plane wave basis states with kinetic energy up to 50 Ryd are used to represent the wave functions. The vacuum region between repeated slabs was larger than 12 Å. Methane is adsorbed on one slab surface only. This procedure avoids errors originating from spurious interactions of adsorbates through the slab. The different work functions of the two slab surfaces are taken into account by allowing for a consistently adjusted discontinuity of the potential in the vacuum region right between the two surfaces.[29]

In the calculations we use the nonspin polarized version of the exchange-correlation functional.[22] The neglect of spin polarization is mainly motivated by the wish to limit the computational costs. It is known that adsorbates, e.g., hydrogen generally reduce the magnetic ordering of nickel.[30] Thus spin polarization is less important for the adsorbed phase. However, the additional stabilization of the clean nickel surface due to magnetic ordering is not taken into account in this calculation. A non-spin-polarized calculation therefore tends to overestimate binding energies (for hydrogen adsorption, for instance, this can be inferred comparing Refs. 30 and Ref. 31).

III. DISSOCIATIVE ADSORPTION OF METHANE ON Ni(111)

A. Isolated H_2 and CH_4 molecules

In order to test the adequacy of the supercell and basis set, we determine the properties of an isolated molecule in the same supercell as used for the surface calculations. Using the gradient-corrected functional and a plane wave cutoff of 70 Ry, we obtain for H_2 the bond length of 0.75 Å and the vibrational quantum of 522 meV. For the binding energy we obtain 4.26 eV including zero-point energy (ZPE) corrections. The experimental values for bond length, vibrational frequency and binding energy (including ZPE) are 0.74 Å, 512 meV, and 4.476 eV, respectively.[32] CH_4 is calculated to have a bond length of 1.09 Å and a vibrational quantum for

TABLE I. Convergence tests for the GGA barrier height $E_b^{CH_4}$ (in kJ/mol) of CH_4 dissociation and for the exothermicity of H_2 dissociation on Ni(111). The number of Ni layers in the slab, N_l, the total number of **k** points, N_k, in the entire Brillouin zone and the plane-wave cutoff E_{cut} (in Ry) are varied.

N_l	N_k	E_{cut}	$E_b^{CH_4}$	$E_{ads}^{H_2}$
4	18	50	108	104
4	18	70	116	···
6	54	50	109	96

the symmetric C–H stretch of 354 meV. The corresponding experimental values are 1.09 Å and 361 meV.

B. Hydrogen on Ni(111)

The stable adsorption site for H on Ni(111) is known to be the three-fold hollow site.[33] In this study, we use an equilibrium distance of 0.93 Å above the surface for the adsorbed H atom in a fcc hollow site. This is slightly smaller than the H-surface distance of 1.18 Å obtained in CI cluster calculations.[33] From experiment, a value of 1.15 ± 0.05 Å has been derived.[34] For H on Ni(110), an increase of the calculated bond length is observed when spin polarization is taken into account.[30,31] Therefore, the discrepancy could be due to our neglect of spin polarization in the present calculation. We find a binding energy of 277 kJ/mol for H in the three-fold hollow site of Ni(111). This is in agreement with density functional calculations for a Ni_{13} cluster, that obtained a binding energy of 272 kJ/mol (Ref. 19, footnote Table VI), and also compares well with a value of 257 kJ/mol from CI cluster calculations.[33] An experimental value for the H chemisorption energy on Ni(111) is 264 kJ/mol, and H_2 dissociation is found to be exothermic by 95 kJ/mol.[35] From the atomic chemisorption energy of hydrogen we calculate that H_2 dissociation is exothermic by 96 kJ/mol (see Table I), not including vibrational zero point corrections.

C. CH_3 on Ni(111)

We find that the three-fold hollow site is the stable adsorption site for CH_3 adsorption on Ni(111) in accord with earlier investigations.[14,15] The carbon atom is located 1.56 Å above the surface. Again, this bond distance is somewhat lower than the result of 1.84 Å from CI cluster calculations.[15] Adsorption on top of a Ni atom, with the carbon atom 1.94 Å above the surface, is 24 kJ/mol higher in energy. In the preferred orientation of the CH_3 group in the hollow site, the hydrogen atoms point towards the Ni atoms. The orientation of the methyl group where the hydrogen atoms point towards the bridges is less favorable by 16 kJ/mol. We calculate a frequency of 16 meV associated with the hindered rotation of the CH_3 group around an axis perpendicular to the surface. In the adsorbed methyl species, the C–H bond length is 1.18 Å. The CH_3 pyramid is somewhat squeezed, with a H–C—H bond angle of $\sim 100°$, compared to 109.5° in CH_4. Taking together the chemisorption energy of a separate H atom and a separate methyl group on Ni(111), we find that the overall

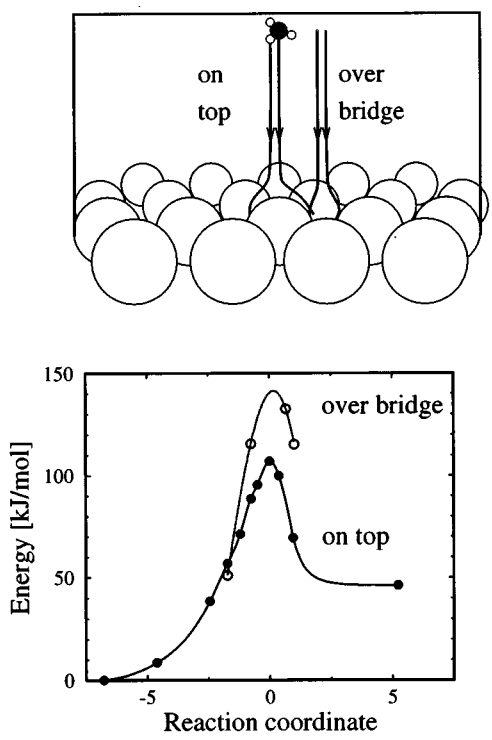

FIG. 1. Potential energy for CH_4 approaching Ni(111) along two possible reaction pathways. Dissociation on top of a Ni atom into opposite hollow sites (full circles) gives rise to a barrier of 108 kJ/mol (not including zero point energies). Dissociation over a bridge site (open circles) is unfavorable because the two adjacent hollow sites are too close together to allow for a stable adsorption of both the hydrogen and the methyl group. Data points were connected by lines to guide the eye.

reaction $CH_4 \rightarrow CH_3^{ads} + H^{ads}$ is endothermic by 18 kJ/mol. Similar findings were reported from density functional calculations on clusters, which obtain an endothermicity for this reaction of 142 and 30 kJ/mol on a Ni_7 and a Ni_{13} cluster, respectively.[19] This is in contrast to CI cluster calculations by Yang and Whitten, who find that the reaction is exothermic by 12 kJ/mol.[16] Experimentally, CH_3 was detected as a reaction product on a surface held at 140 K, after exposure to a beam of CH_4 molecules with translational energy of 71 kJ/mol.[2] This demonstrates that the methyl species is at least metastable, but does not rule out an endothermic adsorption process.

D. Reaction pathway

We have restricted our investigations to reaction pathways where the center of mass of the CH_4 molecule moves in a (112) plane (see Fig. 1) perpendicular to the surface intersecting both the fcc and hcp hollow sites. These sites are the final adsorption sites for H and CH_3. We further assume that the (112) plane is a mirror plane containing the C–H bond that is disrupted during dissociation.

We have studied the interaction of adsorbed H and CH_3 in two adjacent hollow sites in the (112) plane. If the hollows are opposite to a Ni atom, the interaction is repulsive by 28 kJ/mol compared to adsorbates infinitely separated on the surface. For CH_3 and H sitting in two hollow sites con-

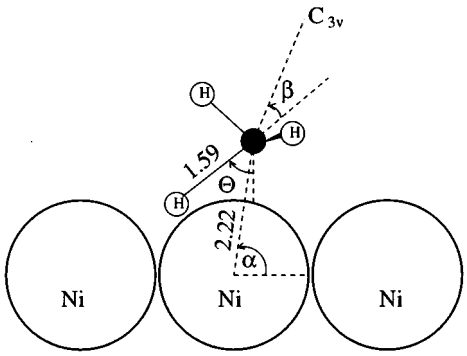

FIG. 2. Geometry of the transition state for dissociation of CH_4 on Ni(111). $\alpha \sim 80°$ and $\Theta = 55°$ denote the orientation of the C–Ni and C–H bond relative to the surface normal. The C_{3v} symmetry axis of the CH_3 group (note that one H atom is hidden) forms an angle $\beta \sim 30°$ with the active C–H bond.

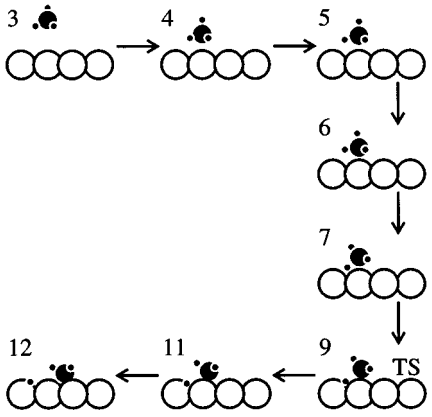

FIG. 3. Selected snapshots during the dissociation of CH_4 on Ni(111). The numbers refer to the geometries listed in Table II.

nected by a bridge, the repulsion is as much as 112 kJ/mol, making this configuration very unstable. Therefore we assume that the most likely pathway for reaction of CH_4 with the Ni(111) surface involves dissociation above a Ni atom into a metastable intermediate state where H and CH_3 are adsorbed in opposite hollow sites next to this Ni atom. This first step will be followed by diffusion of H and diffusion and/or further dissociation of the CH_3 group on the surface.

The transition state of CH_4 dissociating on top of a surface Ni atom has been examined in further detail. Apart from the required $(\bar{1}12)$ mirror symmetry plane, all molecular degrees of freedom of CH_4 are included in the transition state search, while the position of the surface Ni atoms are held fixed. The atomic configuration in the transition state complex is shown in Fig. 2. The active C–H bond is not oriented parallel to the surface, but forms an angle of $\Theta = 55°$ with the surface normal. This is in contrast to H_2 dissociation on (111) surfaces, where the transition state is oriented parallel to the surface. The C–H bond has been stretched to 1.59 Å at the transition state, as compared to 1.09 Å in the CH_4 molecule. The carbon atom has formed a bond with the surface Ni atom that is 2.22 Å long and tilted away from the surface normal. The potential energy surface is rather flat with respect to the tilt and therefore it is difficult to obtain a precise value for this tilt angle α. From our data we estimate $\alpha = 80 \pm 10°$. The orientation of the methyl group with respect to the active C–H bond is different from the free molecule. The transition state configuration corresponds to a bending of the active C–H bond by $\beta \sim 30°$ relative to the C_{3v} symmetry axis of CH_3. To summarize, a sizable amount of deformation of the CH_4 molecule, both bond stretching and bond bending, is required to promote dissociation. This has important dynamical consequences to be discussed later.

Once the transition state has been determined, we may use a strongly damped dynamics to let the transition state complex ''creep down'' to the initial or final state of the reaction. Snapshots along the reaction pathway are obtained in this way. A series of such snapshots is shown in Fig. 3: The molecule approaches the surface above a nickel atom with three C–H bonds pointing towards the surface. To access the transition state, the molecule is reoriented so that one bond is tilted towards the surface, while two others are almost parallel to the surface plane. At the transition state the active C–H bond gets stretched and reoriented towards the adjacent hollow site, while the CH_3 radical retains its orientation relative to the surface. Finally both the H and CH_3 group reach their equilibrium positions, and the adsorbed CH_3 radical reorients itself such that all three C–H bonds point away from the surface. To plot the potential energy along such a sequence of snapshots, we introduce a mass-weighted reaction coordinate s. All masses are measured in units of the mass of a hydrogen atom, m_H. Thus the total mass of CH_4 is $M = 16$, while the reduced mass of the active H atom relative to the methyl radical is $\mu = 0.9375$. Each configuration is described by the position of the carbon atom relative to the surface, $\mathbf{X} = (X,Y,Z)$, and the distance vector from the carbon to the active hydrogen, $\mathbf{x} = (x,y,z)$. A mass-weighted six-dimensional ''distance'' between configurations is introduced by $\Delta s = [M(\Delta X^2 + \Delta Y^2 + \Delta Z^2) + \mu(\Delta x^2 + \Delta y^2 + \Delta z^2)]^{1/2}$. The reaction coordinate s is the sum of small displacements Δs, starting from $s = 0$ at the transition state. Figure 1 shows a plot of the potential energy along the reaction coordinate. The potential governs the motion of a fictitious particle of mass m_H moving along the multidimensional reaction path.

E. Normal modes at the transition state

The CH_4 molecule as a whole has 15 degrees of freedom, consisting of three translational, three rotational, and nine internal coordinates. To simplify the analysis, we will treat the methane molecule in this paragraph as a dimer $H–CH_3$. In this way we may split the nine overall internal modes into six internal modes of CH_3, which will not be considered here, and three remaining modes of the active C–H bond. These are two bending modes of H relative to the CH_3 pyramid, and one stretch mode. The internal CH_3 modes were studied previously in the literature. A softening of these modes during adsorption has been found.[6] It has been explained as due to charge donation from the surface

TABLE II. Potential energy and geometry for a CH_4 molecule dissociating on top of a Ni atom for selected configurations along the reaction path. R_{NiC} is the distance between the active Ni atom and the carbon atom in CH_4 and $R_{CH_{act}}$ is the bond length of the active C–H bond. A graphical representation of the configurations is given in Fig. 3. For the definition of the angles α, β, and Θ, see Fig. 2.

No.	R_{Nic} (Å)	$R_{CH_{act}}$ (Å)	α deg	Θ deg	β deg	E (kJ/mol)
1	∞	1.09	...	...	0	0
2	3.61	1.10	90	73	0	0.2
3	3.06	1.11	90	73	6	8.7
4	2.52	1.11	90	73	6	38.6
5	2.34	1.11	90	73	6	56.9
6	2.22	1.11	89	70	10	71.4
7	2.12	1.29	88	50	15	88.8
8	2.13	1.45	85	54	31	95.5
9	2.06	1.59	79	56	29	108
10	2.04	1.72	81	59	36	100
11	1.98	2.13	78	59	49	69.5
12	2.19	2.93	50	75	74	46.3
13	...	∞	...	90	90	18.3

TABLE III. Frequencies of the normal modes of the transition state complex on the Ni(111) surface. The labeling of the modes refers to the main contribution in the respective eigenvector. Numbers quoted refer to the mass of a hydrogen atom.

Normal mode	TS $\hbar\omega$ (meV)	CH_4 $\hbar\omega$ (meV)
In $(\overline{112})$ plane		
C–H stretch	i110	362
C–H orientation (Θ)	270	0
$(\underline{111})$ translation	70	0
$(\overline{110})$ translation	$<$10	0
C–H bending (β)	80	189
Out of $(\overline{112})$ plane		
C–H bending	50	162
$(\underline{\overline{112}})$ translation	$<$10	0
wagging	40	0
rotation (111) axis	$\sim$0	0
Σ	530	713

into the methyl group,[14] or alternatively by a displacement of the methyl radical away from the hollow site that brings one H atom into a Ni atop position.[15]

Thus we are left with 9 degrees of freedom of the H–CH_3 dimer, that may be decomposed into three translations, three rotations, and three orientations of the CH_3 radical relative to the C–H bond. The calculations presented here concentrate on four coordinates, the motion of the C atom and active H atom in the $(\underline{\overline{112}})$ plane, which are strongly coupled. The following procedure is employed: We calculate the total energy for some 30 test configurations close to the transition state in this four-dimensional subspace and fit it to second-order polynomials. The four normal modes are determined by diagonalizing the dynamical matrix. Only one further mode, excitations in the bending angle β, obeys mirror symmetry in the $(\underline{\overline{112}})$ plane. Further, there are four symmetry-breaking modes, which we assume as decoupled from each other and from the remaining modes. Their frequencies have been determined independently from configurations slightly displaced from the transition state configuration.

The results of the analysis are summarized in Table III. The reaction coordinate, associated with an imaginary frequency of 110 meV, is almost purely a C–H stretch. The highest real mode corresponds to changes in Θ, i.e., in orientation of the C–H bond relative to the surface. This mode involves motion of the active hydrogen atom, leading to a high vibrational quantum. We find several soft modes: the translations of the transition state parallel to the surface, and a rotation around an axis pointing away from the surface. In particular, we have compared two possible transition state complexes that differ by a 90° rotation around the surface normal: In the first case the active C–H bond points to the hollow site, in the second it points to a bridge site between two nickel atoms. We find a negligible energy difference for these two situations. Our results are in qualitative agreement with the vibrational frequencies at the transition state of CH_4 on a Ni_{13} cluster:[19] Here, the reaction coordinate was determined to be mainly a C–H stretch with i108 meV. The authors report real modes at 80 and 45 meV, and several soft modes. The highlying mode associated with the active C–H bond orientation was not included in their analysis (see Ref. 18).

In the present calculation, the sum of all real modes at the transition state (530 meV) is considerably lower than the sum of the corresponding modes in the free molecule (725 meV). This results in a zero point correction to the calculated barrier height of approximately -10 kJ/mol (-100 meV). In the free CH_4 molecule, there are nine additional modes that map onto internal modes of the CH_3 group at the transition state. The sum of their vibrational quanta amounts to 1625 meV. It is therefore conceivable that a slight softening of the internal CH_3 modes at the transition state, we have neglected so far in our analysis, could give an additional (negative) zero point correction to the barrier height.

F. The role of molecular orientation

During the normal mode analysis at the transition state we have encountered two kinds of orientational effects: Lateral corrugation, i.e., rotations around the surface normal have little effect on the energetics. However, the angle between the C–H bond broken during adsorption and the surface normal is important for the efficiency of the bond breaking. Does this mean that only a small fraction of the incoming flux of molecules with the correct bond orientation will dissociate, or do steering forces exist which drive the molecule into the favorable orientation for sticking? In a recent dynamical study on the basis of a LEPS potential for the molecule-surface interaction, Jansen and Burghgraef[20] find that including a rotational degree of freedom reduces the sticking coefficient by about a factor of five. Further, they report a strong tendency to de-excite rotationally excited

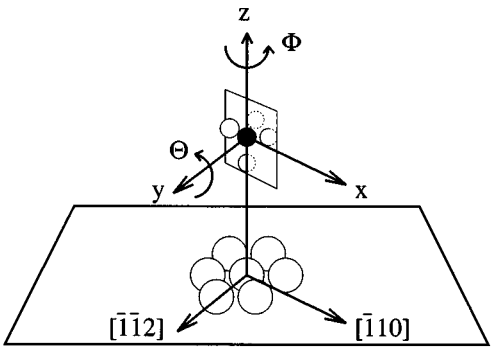

FIG. 4. Illustration of the angles Θ and Φ used to define the orientation of CH_4 relative to the surface.

CH_4 in collisions with the surface. For H_2 dissociation, similar considerations concerning the sticking dependence on impact parameter have been addressed by Darling and Holloway[36] and by Gross *et al.*[37,38]

In order to determine the torque exerted on the molecule, we calculate the potential energy of a rigid CH_4 molecule on top of a nickel atom for various high symmetry orientations of the molecule. The carbon atom is placed at a distance of 2.34 Å above the Ni atom, and all C–H bonds are kept fixed at the equilibrium bond length of 1.09 Å. The orientation of the C–H bond relative to the surface normal is denoted by an angle Θ. The value $\Theta=0$ corresponds to a molecule with one of its H atoms pointing directly towards a nickel atom. Changes in orientation are achieved by a rotation with angle Θ around the $(\bar{1}\bar{1}2)$ axis, followed by a rotation with Φ around the z-axis perpendicular to the surface (see Fig. 4 for illustration). The results for the high symmetry configurations shown schematically in Fig. 5 are summarized in Table IV. We find that the CH_4 molecule is strongly repelled if one of its H atoms points directly towards the nickel atom. In the most favorable configurations, two hydrogen atoms point towards the bridge or hollow sites next to the active Ni atom. There is a sizeable difference in energy between the most favorable and unfavorable configurations, up to 80 kJ/mol. We therefore expect that rotational steering effects play a role in CH_4 dissociation.

Note that the two configurations with $\Theta=125.4°$ and $\Theta=-54.6°$ can be mapped onto each other by a rotation with $\Phi=90°$. Thus the energy difference of 4.5 kcal/mol is a measure for the lateral corrugation, i.e., for the difference between the hydrogens pointing to hollow sites or bridge sites on the surface. Again, we find the effect of lateral corrugation to be small.

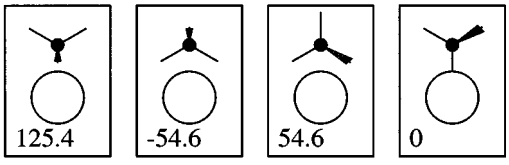

FIG. 5. Schematic illustration of the four molecular orientations in Table IV.

TABLE IV. Energy differences for different orientations of a rigid CH_4 molecule 2.34 Å outside a Ni(111) surface placed on top a Ni atom. For illustration of the molecular configurations, see Fig. 5.

Θ	ΔE (kJ/mol)
125.4	0
−54.6	4.5
54.6	8.3
35.4	17
0	80

G. Discussion

From the calculations presented here we conclude that the barrier for CH_4 dissociation on a static Ni(111) surface is about 100 kJ/mol, including zero point corrections. This value is higher than the barriers of roughly 70 kJ/mol found in CI calculations for Ni(111)[16] and Ni(100),[21] but lower than the results of nonlocal density functional calculations on clusters.[19]

In order to make contact with experimental observations, we can compare our results to data from molecular beam experiments and thermal adsorption experiments. In principle, beam experiments allow the extraction of more information about the dissociation process. The elongated C–H bond we find at the transition state is clearly in qualitative agreement with the strong vibrational enhancement of sticking that is experimentally observed. Further, from our calculations we also expect a contribution to sticking from excitation of the bending modes of the molecule. Because of the strong contribution of molecular excitation to sticking, however, an extraction of the barrier height in the ground state from molecular beam data is difficult. Lee, Yang, and Ceyer found that sticking of CH_4 from a nozzle beam at 640 K is below the detection limit of $S\sim5\times10^{-6}$ at a translational energy of 50 kJ/mol, but rises by two orders of magnitude for a translational energy of 70 kJ/mol. Internal excitation of the molecule was found to be at least as efficient as translational energy. In an attempt to describe their data within a one-dimensional tunneling model, they obtain a barrier height of 109 kJ/mol. Recent measurements of Holmblad, Larsen, and Chorkendorff[3] at nozzle temperatures of 550 and 1050 K are in agreement with the earlier data of Lee *et al.* At the lowest translational energies used, around 50 kJ/mol, the sticking coefficients at $T_{noz}=550$ K and $T_{noz}=1050$ K differ by two orders of magnitude. This suggests that sticking at these translational energies is dominated by molecules with one C–H stretch quantum excited (and possibly one quantum in the bending mode, too). To determine the adsorption barrier for molecules in the ground state, an internal-state-resolved analysis of the data is required. Holmblad, Wambach, and Chorkendorff[5] have performed this type of analysis for sticking on Ni(100) for a scenario where only the C–H stretch mode (quantum number ν_1) is assumed to be important. From a parametrization of their data they obtain sticking coefficients as function of kinetic energy for the three lowest vibrational states. These curves (cf. Ref. 5, Fig. 10) show that sticking at the 1% level for molecules in the

states $\nu_1=0$, $\nu_1=1$, and $\nu_1=2$ sets in at translational energy thresholds of 90, 40, and 15 kJ/mol, respectively. Internal-state-resolved data for Ni(111) is not yet available. We expect similar thresholds for Ni(111), though slightly higher, because sticking factors for CH_4 on Ni(111) are generally somewhat lower than on Ni(100).

The activation energies for CH_4 adsorption on nickel surfaces from a thermal gas are generally lower than the thresholds discussed above, in the range of 50–60 kJ/mol.[9,10] However, as has been pointed out earlier by Luntz and Harris,[7,8] caution is required when comparing activation energies to calculated barrier heights. For example, an onset of sticking at ~90 kJ/mol for molecules in the ground state, as we reported above for Ni(100), is not necessarily at variance with the measured apparent activation energy for CH_4 adsorption from a thermal gas. The parametrization used in Ref. 5 reproduces the apparent activation energy of 52 kJ/mol of Ref. 10. This is possible because of a sizeable contribution from excited states to the sticking coefficient of a thermal gas, and the large energy width of the state-specific sticking functions used to parametrize the beam data. Lee and Ceyer have tentatively assumed that tunneling of the active H atom through the barrier is responsible for the width of the sticking functions. Isotope experiments show that the sticking is a factor 5–10 lower for CD_4 than for CH_4, both on Ni(111)[2] and on Ni(100).[5] However, experimentally, the logarithmic slope of the sticking curve, $d(\log s)/dE=0.19\pm0.02\ \mathrm{kJ}^{-1}$ mol is identical for both CH_4 and CD_4 within the experimental error margin. This is at variance with a simple one-dimensional tunneling model which would predict a factor 2 difference in the slopes. From the thickness of the calculated barrier, we can estimate the contribution of one-dimensional tunneling to the energetic width of the sticking function. Using the imaginary mode $\hbar\omega=110$ meV and the WKB expression for tunneling through a parabolic barrier, we obtain $d(\log s)/dE=2\pi/(\hbar\omega)=0.59\ \mathrm{kJ}^{-1}$ mol for CH_4 and 1.18 kJ^{-1} mol for CD_4. The sticking curve deduced from the calculated potential via a one-dimensional tunneling model rises too steep compared to the experimental curve. Stated with other words, one-dimensional tunneling can only partially account the energetic width of the sticking function. More detailed dynamical calculations including three degrees of freedom[20] find that a one-dimensional tunneling model is not a particularly good description of the dynamics. However, even their 3D dynamical model gives an energetic width too small compared to experiment. Recent model calculations by Luntz for Ni(100)[8] attribute part of the width to a distribution of barriers encountered by molecules in different internal configurations. These calculations also suggest that the isotope effect is mostly due to different vibrational zero point energies for CH_4 and CD_4. We therefore speculate, that more complicated dynamics in a higher-dimensional configuration space, i.e., tunneling combined with redistribution of internal energy within the molecule, could be active in CH_4 adsorption dynamics. This is already the case for the much simpler molecule, H_2, see for instance Refs. 36, 37, 38, 39, 40, and 41.

We further note, that the dissociation barrier calculated for a *static* surface might not be completely adequate to the experimental situation in sticking. A nickel atom is about three times heavier than a CH_4 molecule. From time scale arguments, we can not exclude that the Ni atoms of the surface have enough time to adjust their positions during an encounter with CH_4. On the contrary, some coupling between the methane and the surface atoms can be inferred from the dependence of sticking on surface temperature observed in the experiments.[5] Earlier work by Luntz and Harris[7] has attributed this surface temperature dependence to a mechanical coupling between the Ni atom and the scattered CH_4 molecule by its recoil.

To conclude this discussion, we note that the calculated barrier height of ~100 kJ/mol is compatible with the results from beam experiments if we assume that internal molecular excitations and tunneling contribute to sticking for the energies used in these beam experiments. At present too little is known about the role of dynamics to give a reliable theoretical determination of the tunneling width. Therefore, the role of tunneling versus thermal excitations in the adsorption of thermal CH_4 remains an open question.

IV. MODIFICATION OF THE REACTIVITY BY ALLOYING

A. Surface alloy with gold

Gold atoms alloyed into the Ni(111) surface offer an ideal system to study the effect of alloying on the chemical reactivity of a catalyst. Although the phase diagram of gold and nickel exhibits a miscibility gap, gold atoms deposited on the Ni(111) surface do not form islands, but substitute nickel atoms in the surface layer. Because of the huge barrier towards gold diffusion into the bulk, the stochiometry of the surface alloy is relatively stable in the presence of reactants and over a range of surface temperatures. STM images allow the determination of the distribution of Au and Ni atoms relative to each other at different Au coverages and thus the statistics of local atomic ensembles on the surface.

Noble metals, in particular gold, are unreactive with respect to CH_4 dissociation. Substituting Ni surface atoms with Au atoms will therefore block at least one active site for CH_4 dissociation, and possibly other sites in the neighborhood of the Au. We investigate how much the barrier for dissociation of CH_4 above a Ni atom changes for Ni atoms that have one or two Au neighbors. In the 4-layer slab described earlier, we replace one of the four Ni atoms in the unit cell of the topmost layer with gold, corresponding to a gold coverage of $\Theta_{Au}=0.25$ ML. Each surface Ni atom now has two Au neighbors and four Ni neighbors. After inserting the Au atom, the positions of all atoms in the two outermost layers of the slab are relaxed. To investigate the properties of a Ni atom with one Au neighbor, we use a 4-layer slab with six atoms in the lateral unit cell. One atom in the unit cell of the surface layer is taken to be a Au atom ($\Theta_{Au}=1/6$ ML). Surface relaxations are taken over from the slab described

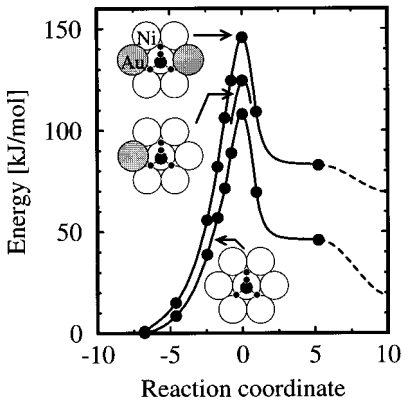

FIG. 6. The calculated energy along the reaction path for CH_4 dissociating over a Ni atom in the Ni(111) surface. Results from similar calculations for dissociation over a Ni atom with one or two Au nearest neighbors are also included. During the reaction the surface atoms are kept fixed at their positions on the corresponding free surfaces. The rightmost data points (dashed curves) refer to infinite separation of the dissociated H and CH_3 group on the surface. The dissociation geometry for the three chemical compositions is indicated by the insets, with gold atoms gray-shaded.

previously. The CH_4 molecule is placed at the transition state above the active Ni atom at the same relative distance and orientation as on the clean Ni(111) surface. The final adsorption sites are hollows surrounded by three Ni atoms in all cases described (see inset in Fig. 6). The potential energies along the reaction path are displayed in Fig. 6. We find that the dissociation barrier is increased relative to the clean Ni(111) surface by $\Delta E_1 = 16$ kJ/mol and $\Delta E_2 = 38$ kJ/mol for a Ni atom with one and two gold neighbors, respectively.

Recently, Holmblad, Larsen, and Chorkendorff[3] performed a molecular beam study on the effect of gold on the sticking of CH_4 on Ni(111). The decrease of the relative sticking coefficient (normalized to its value on the clean surface) was measured as a function of gold coverage. The data is analyzed in terms of local ensembles consisting of seven atoms, one central Ni atom surrounded by a ring of six neighbors, which may be either Ni or Au. The probability p_N of finding a particular ensemble consisting of a Ni atom with N gold neighbors on the alloyed surface is known from STM images for various gold coverages.[42] For gold atoms distributed randomly on the surface, one obtains

$$p_N(\Theta_{\mathrm{Au}}) = \frac{6!}{N!(6-N)!}\Theta_{\mathrm{Au}}^N(1-\Theta_{\mathrm{Au}})^{(7-N)}. \tag{1}$$

Probabilities calculated with this simplifying assumption already give a close description of the experimentally determined ensemble probabilities. The normalized sticking coefficient as a function of gold coverage may then be written

$$s(\theta_{\mathrm{Au}})/s_0 = p_0(\theta_{\mathrm{Au}}) + p_1(\theta_{\mathrm{Au}})s_1/s_0 + p_2(\theta_{\mathrm{Au}})s_2/s_0 + \cdots . \tag{2}$$

Here, s_1/s_0 and s_2/s_0 denote the relative sticking coefficient at sites with one and two Au neighbors, respectively. The ratios s_N/s_0 can be directly compared to the calculated changes in barrier height ΔE_N, independent of the details of the adsorption dynamics. We only have to assume that sticking is solely determined by the kinetic energy E_T of the incoming molecule *relative* to the barrier height, if the degree of internal excitation of the molecule is unchanged. For sites with a barrier which is ΔE_N higher than for pure Ni(111), we then get $s_N/s_0 = s_0(E_T - \Delta E_N, T_{\mathrm{noz}})/s_0(E_T, T_{\mathrm{noz}})$ at a given nozzle temperature T_{nozz} and beam kinetic energy E_T. In Table V, values for s_N/s_0 derived by using the calculated ΔE_N and the sticking functions (Ref. 3, Fig. 5) are compared to the experimental values obtained directly from fitting the measured $s(\Theta_{\mathrm{Au}})/s_0$ to the form of Eq. (2) (cf. Ref. 3). The good agreement shows that the density functional calculations accurately describe the differences in barrier height for Ni atoms in chemically different environments.

TABLE V. Relative sticking coefficient of methane, s_N/s_0, for Ni atoms with N Au neighbors, normalized to the sticking coefficient on the pure Ni(111) surface, s_0. Numbers in the first column are obtained by fitting experimental data of Ref. 3 to the ensemble model expressed in Eq. (2). The second column gives the numbers predicted from the calculated barrier heights on the basis of the measured energy dependence of the sticking coefficient.

		Expt.	Theor.
s_1/s_0	$T_{\mathrm{noz}} = 550$ K	0	0.07
s_1/s_0	$T_{\mathrm{noz}} = 1050$ K	0.27	0.22
s_2/s_0	$T_{\mathrm{noz}} = 550$ K	0	<0.001
s_2/s_0	$T_{\mathrm{noz}} = 1050$ K	0	0.026

The ratios s_N/s_0 also contain interesting information about the dynamics of adsorption. If we take the point of view that the total sticking can be decomposed into contributions from molecules in different vibrational states related to the C–H stretch, the numbers of Table V together with the calculated barrier height suggest that the translational energy used in this particular experiment, about 75 kJ/mol, is slightly higher than the translational energy threshold for the $\nu_1 = 1$ state, but clearly above the threshold for $\nu_1 = 2$. At the lower nozzle temperature, molecules with multiple vibrational excitations in the beam are rare, and the sticking is determined by molecules in the $\nu_1 = 1$ state alone which have just enough energy to overcome the barrier. This contribution to the sticking is very sensitive to the barrier height, and already a slightly increased barrier, as is found for Ni atoms with one Au neighbor, inhibits sticking efficiently. At high nozzle temperature, strongly vibrationally excited molecules contribute significantly to the sticking. Since their energy clearly exceeds the barrier height, they contribute to the overall sticking factor even at the Ni sites with one gold neighbor. The barrier at sites with two Au neighbors is too high to give any significant contribution to sticking even from highly excited molecules.

In summary, the modelling by statistical ensembles combined with the knowledge of ΔE_N allows the reproduction of the whole function $s(\Theta_{\mathrm{Au}})/s_0$ solely from the energy dependence of the sticking curve. This was demonstrated already in an earlier publication.[42] Fig. 4 in Ref. 42 clearly shows that the model developed above quantitatively describes not

only the variation of the sticking probability with the Au content of the surface, but also the variations with the nozzle temperature T_{noz}. Although we have used ensembles to model the adsorption, the effect described here should not be confused with the well-known ensemble effect in reaction kinetics. The effect reported here is rather due to a change in electronic structure at the active Ni atom (i.e., comparable to what is usually called a ligand effect in physical chemistry). We note that the effect of alloying can also increase the reactivity of nickel in some cases. For the same transition state configurations as used above, but on top of a Ni atom at a substitutional site in a Cu(111) surface, we find a barrier for methane dissociation which is 0.05 eV lower than on the clean Ni surface. The same trend has been observed in experiments on bulk alloy catalysts made of nickel with moderate admixtures of copper.[43]

B. The role of the nickel *d* states

It is possible to relate the effect of alloying on the dissociation barrier of CH_4 to the general ability of transition metals to catalyze surface reactions. Dissociation of CH_4 is frequently described as oxidative addition of nickel to a C–H bond. This means that the nickel surface provides electronic states near the Fermi level (from the partially occupied d band) that may ''substitute'' molecular states in the course of adsorption. To visualize this effect from the calculations, we define a bonding orbital $|\sigma\rangle$ and an antibonding orbital $|\sigma^*\rangle$ for the active C–H bond by symmetric or antisymmetric linear combination of the hydrogen $1s$ orbital with a suitably chosen $2sp^3$ orbital of carbon. To assess the role of the nickel surface in breaking the C–H bond, the relevant quantity is the density of states weighted by the overlap population of this bond.[44] This orbital-projected density of states,

$$p_\sigma(E)=\sum_{i,\mathbf{k}} (|\langle\Psi_{i\mathbf{k}}(E)|\sigma\rangle|^2-|\langle\Psi_{i\mathbf{k}}(E)|\sigma^*\rangle|^2),$$

is plotted for the transition state of CH_4 dissociation in the right panel of Fig. 7. Here $\Psi_{i\mathbf{k}}$ are the calculated wave functions for the adsorption system at the transition state, with the indices i and $\mathbf{k}$ denoting the sum over occupied bands and over the Brillouin zone, respectively. In the left panel, the density of states projected onto the $3d$ states $|nlm\rangle=|32m\rangle$ of a nickel atom at a free surface are shown for comparison, i.e., the quantity

$$p_d(E)=\sum_{m=-2}^{+2}\sum_{i,\mathbf{k}} |\langle\Psi_{i\mathbf{k}}(E)|32m\rangle|^2.$$

The graphs show that the overlap between the hydrogen $1s$ and carbon $2sp^3$ orbital acquires antibonding character in the range of energies of the nickel *d* band. In other words, an antibonding level of the CH_4 molecule starts to interact with the nickel *d* states and partially evolves into a *d*-band resonance as the molecule approaches the surface. The mixing of the antibonding orbital with the *d*-band lowers the energy of the transition state and finally leads to dissociation. The interaction of the bonding orbital with the *d* states will further stabilize the transition state.

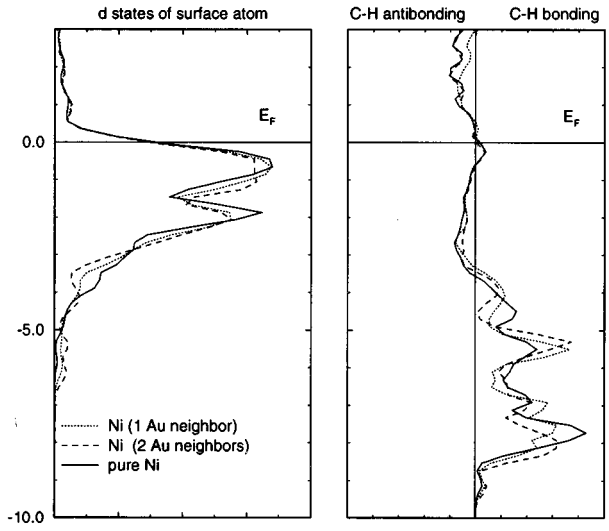

FIG. 7. Left panel: p_d, the density of states (in arbitrary units) projected onto the d orbitals of a nickel atom with zero, one and two gold neighbors (full, dotted, and dashed line) on the clean alloy surface. Right panel: p_σ, the density of states projected onto the bond overlap of the active C–H bond at the transition state at nickel atoms in the different chemical environments. The Fermi energy has been chosen as common zero of the energy scale. The center of the *d* states is lowered by the presence of gold atoms. As a result, the interaction of the molecular antibonding level with the d states decreases with the number of gold neighbors and the transition state is less tightly bound.

From such a picture of dissociative adsorption it is plausible that the position of the center of the *d* states is a key quantity for the ability of a surface metal atom to promote dissociation. Interaction with the unoccupied antibonding molecular state is favored by a narrow and high-lying band of *d* states. From this argument, trends in the dissociation barrier on an alloy surface above atoms in chemically different environments can be estimated by looking at the *d*-state profiles of the relevant atoms. Figure 7 displays the situation for nickel atoms with zero, one, or two gold neighbors in the alloy. The lowering of the *d* states for an increasing number of gold neighbors correlates with the rise of the dissociation barrier. The center of the *d* states, defined by

$$E_d^c=\int_{-\infty}^{E_F} E p_d(E)dE \Big/ \int_{-\infty}^{E_F} p_d(E)dE$$

is lowered relative to the pure nickel surface by 15 and 46 meV for Ni atoms with one and two gold neighbors, respectively. Simultaneously, the dissociation barrier for CH_4 rises by 16 and 38 kJ/mol, respectively. The density of states projected onto the C–H bond overlap (right panel of Fig. 7) illustrates this trend. Due to the weaker interaction between the σ^* level and the *d* states of the surface atom with increasing gold concentration, the transition state complex becomes less tightly bound to the surface. This is in qualitative agreement with the role of σ^*-d interaction for the dissociation of H_2 on late transition and noble metals.[45]

V. CONCLUSIONS

Using gradient-corrected density functional calculations for dissociative adsorption of CH_4 and a slab model of the Ni(111) surface we find a barrier of about 100 kJ/mol (including zero-point corrections) for the rupture of the C–H bond. The transition state involves considerable bond stretch and deformation of the molecule in qualitative agreement with the experimental observation that molecular excitations promote sticking of CH_4 efficiently. The calculated barrier height is compatible with the results from beam experiments if we assume that internal molecular excitations and tunneling contribute to sticking for the energies used in these beam experiments. A normal mode analysis shows that the reaction proceeds mainly through a stretch of the C–H bond, but the C–H bond orientation is also important and steering forces exist that drive the molecule to an orientation most favorable for adsorption. The role of nickel in catalyzing the dissociation of CH_4 is due to its high density of *d*-states close to the Fermi level. The effect of electronic structure on dissociation has been studied for the nickel–gold surface alloy system for various admixtures of gold. The local density of *d*-states at a reactive nickel atom is lowered energetically when the number of its gold neighbors increases, accompanied by a rise in the barrier for CH_4 dissociation. We have shown that the normalized sticking probability for a Ni–Au alloy of arbitrary composition can be obtained from the calculated variation of the local barrier in the alloy surface and the energy dependence of sticking. Within a simple statistical model based on ensembles of atoms on the alloy surface we demonstrate that the local reactivity of an atom in the ensemble is influenced by its neighbors via electronic effects. The resulting variation in barrier height can be accurately predicted by density functional calculations.

ACKNOWLEDGMENTS

Center for Atomic-scale Materials Physics is sponsored by the Danish National Research Foundation. The present work was in part financed by The Center for Surface Reactivity under the Danish Research Councils. The calculations have only been possible due to the computational resources of the JRCAT supercomputing system, which is supported by the New Energy and Industrial Technology Development Organization (NEDO) of Japan. We would like to thank I. Chorkendorff, A. C. Luntz, W. Brenig, M. Holmblad, and J. Hvolbaek Larsen for discussions.

[1] J. R. Rostrup-Nielsen, *Catalytic Steam Reforming*, Vol. 5 of *CATALYSIS - Science and Technology* (Springer, Berlin, 1984).
[2] M. B. Lee, Q. Y. Yang, and S. T. Ceyer, J. Chem. Phys. **87**, 2724 (1987).
[3] P. M. Holmblad, J. H. Larsen, and I. Chorkendorff, J. Chem. Phys. **104**, 7289 (1996).
[4] A. V. Hamza and R. J. Madix, Surf. Sci. **179**, 25 (1987).
[5] P. M. Holmblad, J. Wambach, and I. Chorkendorff, J. Chem. Phys. **102**, 8255 (1995).
[6] S. T. Ceyer *et al.*, J. Vac. Sci. Technol. **A 5**, 501 (1987).
[7] A. C. Luntz and J. Harris, Surf. Sci. **258**, 397 (1991).
[8] A. C. Luntz, J. Chem. Phys. **102**, 8264 (1995).
[9] T. P. Beebe, Jr., D. W. Goodman, B. D. Kay, and J. T. Yates, Jr., J. Chem. Phys. **87**, 2305 (1987).
[10] I. Chorkendorff, I. Alstrup, and S. Ullmann, Surf. Sci. **227**, 291 (1990).
[11] L. Hanley, Z. Xu, and J. T. Yates, Jr., Surf. Sci. **248**, L265 (1991).
[12] M. R. A. Blomberg, U. Brandemark, and P. E. M. Siegbahn, J. Am. Chem. Soc. **105**, 5557 (1983).
[13] A. B. Anderson and J. J. Maloney, J. Phys. Chem. **92**, 809 (1988).
[14] J. Schüle, P. Siegbahn, and U. Wahlgren, J. Chem. Phys. **89**, 6982 (1988).
[15] H. Yang and J. L. Whitten, J. Am. Chem. Soc. **113**, 6442 (1991).
[16] H. Yang and J. L. Whitten, J. Chem. Phys. **96**, 5529 (1992).
[17] H. Burghgraef, A. P. J. Jansen, and R. A. van Santen, J. Chem. Phys. **98**, 8810 (1993).
[18] H. Burghgraef, A. P. J. Jansen, and R. A. van Santen, Faraday Discuss. Chem. Soc. **96**, 337 (1993).
[19] H. Burghgraef, A. P. J. Jansen, and R. A. van Santen, J. Chem. Phys. **101**, 11 012 (1994).
[20] A. P. J. Jansen and H. Burghgraef, Surf. Sci. **344**, 149 (1995).
[21] O. Swang, J. K. Faegri, O. Gropen, U. Wahlgren, and P. E. M. Siegbahn, Chem. Phys. **156**, 379 (1991).
[22] J. P. Perdew *et al.*, Phys. Rev. B **64**, 6671 (1992).
[23] D. M. Ceperley and B. J. Alder, Phys. Rev. Lett. **45**, 566 (1980).
[24] J. P. Perdew and A. Zunger, Phys. Rev. B **23**, 5048 (1981).
[25] M. C. Payne, M. P. Teter, D. C. Allan, T. A. Arias, and J. D. Joannopoulos, Rev. Mod. Phys. **64**, 1045 (1992).
[26] M. J. Gillan, J. Phys.: Condens. Matter **1**, 689 (1989).
[27] N. Troullier and J. L. Martins, Phys. Rev. B **43**, 1993 (1991).
[28] L. Kleinman and D. M. Bylander, Phys. Rev. Lett. **48**, 1425 (1982).
[29] J. Neugebauer and M. Scheffler, Phys. Rev. B **46**, 16 067 (1992).
[30] M. Weinert and J. W. Davenport, Phys. Rev. Lett. **54**, 1547 (1985).
[31] C. Umrigar and J. W. Wilkins, Phys. Rev. Lett. **54**, 1551 (1985).
[32] K. P. Huber and G. Herzberg, *Molecular Spectra and Molecular Structure* (Van Nostrand–Reinhold, New York, 1979).
[33] H. Yang and J. L. Whitten, J. Chem. Phys. **89**, 5329 (1988).
[34] K. Christmann, R. J. Behm, G. Ertl, M. A. V. Hove, and W. H. Weinberg, J. Chem. Phys. **70**, 4168 (1979).
[35] K. Christmann, O. Schober, G. Ertl, and M. Neumann, J. Chem. Phys. **60**, 4528 (1974).
[36] G. R. Darling and S. Holloway, Surf. Sci. **304**, L461 (1994).
[37] A. Gross, B. Hammer, M. Scheffler, and W. Brenig, Phys. Rev. Lett. **73**, 3121 (1994).
[38] A. Gross, S. Wilke, and M. Scheffler, Phys. Rev. Lett. **75**, 2718 (1995).
[39] S. Holloway and G. Darling, Rep. Prog. Phys. **58**, 1595 (1995).
[40] P. Kratzer, B. Hammer, and J. K. Nørskov, Surf. Sci. **359**, 45 (1996).
[41] G. J. Kroes, G. Wiesenekker, E. J. Baerends, and R. C. Mowrey, Phys. Rev. B **53**, 10397 (1996).
[42] P. M. Holmblad *et al.*, Catal. Lett. (in press).
[43] I. Alstrup and M. T. Tavares, J. Catal. **139**, 513 (1993).
[44] J.-Y. Saillard and R. Hoffmann, J. Am. Chem. Soc. **106**, 2006 (1984).
[45] B. Hammer and J. K. Nørskov, Surf. Sci. **343**, 211 (1995); Surf. Sci. **359**, 306 (E) (1996).